

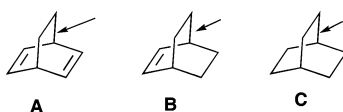
# Manifestations of the Alder–Rickert Reaction in the Structures of Bicyclo[2.2.2]octadiene and Bicyclo[2.2.2]octene Derivatives

Yit Wooi Goh, Stephen M. Danczak, Tang Kuan Lim, and Jonathan M. White\*

School of Chemistry and Bio-21 Institute, The University of Melbourne,  
Parkville Vic 3010 Melbourne, Australia

whitejm@unimelb.edu.au

Received December 13, 2006



The C–C bond distances from the bridgehead to the ethylene fragment in molecules containing the moieties A and B are lengthened compared to saturated analogs containing the fragment C. These structural effects are consistent with manifestation of the Alder Rickert Reaction in the Ground State

The Alder–Rickert ethylene extrusion reaction manifests in the ground state structures of compounds **9–12** which contain the bicyclo[2.2.2]octadiene moiety and compounds **13, 14**, and **17–20** which contain the bicyclo[2.2.2]octene moiety. A significant decrease of the  $^{13}\text{C}$ – $^{13}\text{C}$  one-bond coupling constants for the C–C bonds, which break in this fragmentation reaction, suggests lengthening, and hence weakening of these bonds. In the unsymmetrical systems these effects are also shown to be associated with strengthening of the  $\text{CH}_2$ – $\text{CH}_2$  bond, which is ultimately lost from the molecule as ethylene. Low-temperature crystal structures of compounds **9–12** and **16** provide evidence for similar crystal packing requirements of the  $\text{CH}_2$ – $\text{CH}_2$  and  $\text{CH}=\text{CH}$  moieties.

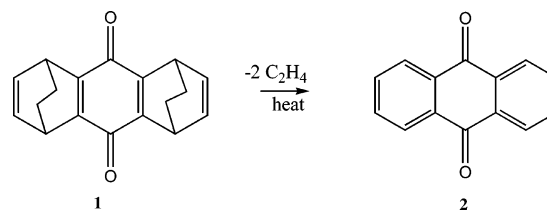
## Introduction

There have been several reports on the decomposition of cycloadducts formally from 1,3-cyclohexadiene and a variety of alkyne dienophiles.<sup>1</sup> These molecules, upon heating, readily lose ethylene, giving rise to a stable aromatic product. Diels, Alder, and co-workers first observed this reaction in 1929, when the oxidized cycloadduct of quinone and 1,3-cyclohexadiene (**1**) gave ethylene and the aromatic quinone (**2**) as shown in Scheme 1.<sup>2</sup>

The facile nature of this reaction and the ease of identifying the aromatic product has led to this reaction being applied as a diagnostic test for the presence of the 1,4-cyclohexadiene moiety, in some unidentified compounds. In addition, this reaction has also been widely used in the synthesis of other aromatic compounds, including derivatives of naphthoquinone and anthraquinone.

The Structure Correlation Principle states that structural changes, which occur along the reaction coordinate, for a

## SCHEME 1



particular reaction can reveal themselves in the ground state as deviations of bond distances and angles from “normal” values along the reaction coordinate.<sup>3</sup> This holds provided that the ground state geometry of the molecule is similar to the transition state geometry for the reaction, as this allows the orbitals, which are involved in the reaction, to mix in the ground state. For example, in cycloadducts formed between a cyclic diene and an alkene dienophile, for which the cyclohexane ring exists in a boat conformation, structural effects consistent with the early stages of the retro-Diels–Alder reaction are clearly apparent.<sup>4</sup> These effects include significant lengthening of the two C–C bonds, which break in the reaction. For example, in the

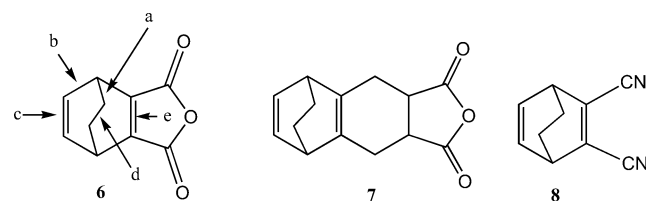
(1) Kanakam, C. C.; Ramanathan, H.; Rao, G. S. R. S.; Birch, A. J. *Curr. Sci.* **1982**, 51, 400–2.

(2) Alder, K.; Stein, G.; Pries, P.; Winckler, H. *Ber. Dtsch. Chem. Ges.* **1929**, 62B, 2337–72.

(3) Burgi, H. B.; Dunitz, J. D. *Acc. Chem. Res.* **1983**, 16, 153.

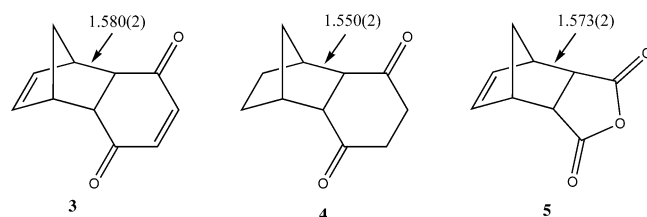
(4) Pool, B.; White, J. M. *Org. Lett.* **2000**, 2, 3505.

TABLE 1. Selected Bond Distances (Å) for Structures 6–8



|   | 6        | 7        | 8        |
|---|----------|----------|----------|
| a | 1.579(2) | 1.558(3) | 1.559(2) |
| b | 1.530(2) | 1.508(2) | 1.512(2) |
| c | 1.350(2) | 1.319(2) | 1.325(2) |
| d | 1.519(2) | 1.540(2) | 1.524(2) |
| e | 1.340(2) | 1.321(2) | 1.346(2) |

cyclopentadiene–benzoquinone adduct **3**, the C–C bonds which break in the retro-Diels–Alder reaction are lengthened by ca. 0.03 Å relative to those in the corresponding saturated derivative **4**, which does not undergo this pericyclic fragmentation.<sup>5</sup> A qualitative relationship between structure and reactivity for this retro-Diels–Alder reaction is suggested when comparison is made between the structural parameters of the reactive adduct **3** with those for the less reactive maleic anhydride cycloadduct **5**.



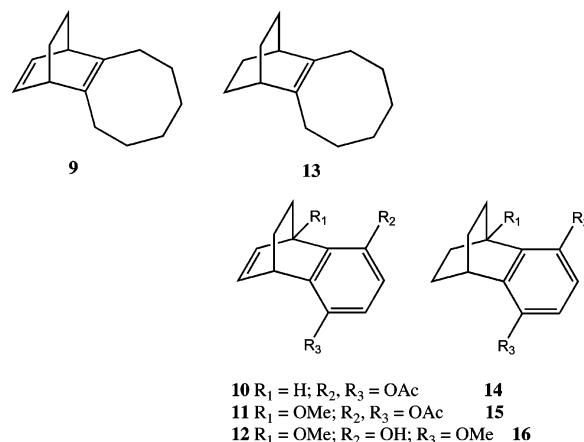
Our aim was to extend our structural studies to encompass adducts which span a wide range of reactivities toward the retro-Diels–Alder reaction, so that a quantitative relationship between structure and reactivity could be established. Such a relationship might allow us to predict reaction rates based on crystal structure data. To this end we chose to undertake a structural study of a variety of (formal) cyclohexadiene–alkyne cycloadducts, which undergo the Alder–Rickert reaction with loss of ethylene. The driving force for this reaction in these adducts which contain the bicyclo[2.2.2]octa-2,5-diene moiety is likely to be strong, as one of the products is aromatic. Therefore, we were interested in studying the structures of these cycloadducts to determine whether the extra driving force for this reaction would result in more pronounced structural effects in the ground state.

As a preliminary to this work, we undertook a search of the Cambridge Crystallographic Database<sup>6</sup> and extracted the structures **6–8**,<sup>7–9</sup> for which relevant structural parameters are summarized in Table 1. While no evidence of ethylene extrusion in monosaturated or fully saturated derivatives has been reported,

compound **6**, which has been reported to exhibit clean ethylene extrusion upon heating at 110 °C for 1 h, showed particularly pronounced structural effects.<sup>10</sup> The mean C–C bond distances from the bridgehead carbon to the ethylene bridge, which breaks in this reaction (bond C<sub>3</sub>–C<sub>9</sub> and C<sub>6</sub>–C<sub>10</sub>), are extremely long (1.579 Å), the C<sub>9</sub>–C<sub>10</sub> distance (1.518 Å) is slightly shorter than a typical C–C single bond, and the C<sub>4</sub>–C<sub>5</sub> distance is longer than a standard C=C double bond.<sup>11</sup> These marked effects are consistent with the changes in bond order which occur along the retro-Diels–Alder reaction coordinate.

However, the structural effects in adducts **7** and **8**, which should be similar, were much less pronounced, suggesting that this class of compounds merit further, careful structural investigation.

The targets for this study were the bicyclo[2.2.2]octadiene derivatives **9–12** which have differing reactivities toward the Alder–Rickert reaction. Compound **9** loses ethylene rapidly at 170 °C<sup>12</sup> while **10–12** require heating at 200 °C for extended periods of time. The differing reactivities of **9** compared to **10–12** probably reflect the greater driving force associated with the formation of a benzene-type aromatic system compared with the formation of a naphthalene-type aromatic system. The partially unsaturated bicyclo[2.2.2]octene analogues **13–16** which have significantly lower reactivity were also chosen so as to extend this structure–reactivity series.



## Results and Discussion

Compound **9** was prepared by reaction between 1,3-cyclohexadiene and cyclooctyne,<sup>12</sup> while compounds **10–12** were prepared by a modification of literature procedures.<sup>13,14</sup> The bicyclo[2.2.2]octene analogues **13–16** were obtained from compounds **9–12** via catalytic hydrogenation. Cycloadducts **10–12**, **14**, and **16** gave crystals of suitable quality for X-ray analysis. X-ray data for **10–12**, **14**, and **16** were collected at low temperature to minimize the unwanted effects of thermal libration.

(5) Birney, D.; Lim, T. K.; Peng, J.; Pool, B. R.; White, J. M. *J. Am. Chem. Soc.* **2002**, *124*, 5091.

(6) Allen, F. H.; Bellard, S.; Brice, M. D.; Cartwright, B. A.; Doubleday, A.; Higgs, H.; Hummelink-Peters, T.; Kennard, O.; Motherwell, W. D. S.; Rogers, J. R.; Watson, D. G. *Acta. Crystallogr.* **1979**, *B35*, 2331.

(7) Irngartinger, H.; Oeser, T.; Jahn, R.; Kallfass, D. *Chem. Ber.* **1992**, *125*, 2067–73.

(8) Pinkerton, A. A.; Schwarzenbach, D.; Birbaum, J. L.; Carrupt, P. A.; Schwager, L.; Vogel, P. *Helv. Chim. Acta* **1984**, *67*, 1136–53.

(9) Williams, R. V.; Todime, M. M. R.; Enemark, P.; van der Helm, D.; Rizvi, S. K. *J. Org. Chem.* **1993**, *58*, 6740–4.

(10) Williams, R. V.; Todime, M. H. R.; Enemark, P.; van der Helm, D.; Rizvi, S. K. *J. Org. Chem.* **1993**, *58*, 6740.

(11) Allen, F. H.; Kennard, O.; Watson, D. G.; Brammer, L.; Orpen, A. G.; Taylor, R. *J. Chem. Soc., Perkin Trans. 2* **1987**, *12*, S1–S19.

(12) Meier, H.; Molz, T.; Merkle, U.; Echter, T.; Lorch, M. *Liebigs. Ann. Chem.* **1982**, 914.

(13) Hugo, V. I.; Nicholson, J. L.; Snijman, P. W.; Green, I. R. *Synth. Commun.* **1994**, *24*, 23–8.

(14) Hugo, V. I.; Snijman, P. W.; Green, I. R. *Synth. Commun.* **1993**, *23*, 577–84.

TABLE 2. Crystal Data and Structure Refinement Details for Compound 10–12, 14, and 16

|  | 10   | 11   | 12   | 14   | 16   |
|--|--|--|--|--|--|
| empirical formula  | C <sub>16</sub> H <sub>16</sub> O <sub>4</sub> | C <sub>17</sub> H <sub>18</sub> O <sub>5</sub> | C <sub>14</sub> H <sub>16</sub> O <sub>3</sub> | C <sub>16</sub> H <sub>18</sub> O <sub>4</sub> | C <sub>14</sub> H <sub>18</sub> O <sub>3</sub> |
| formula weight   | 272.29   | 302.31   | 232.27   | 274.30   | 234.28   |
| temperature (°C)   | 130(2)   | 130(2)   | 130.0(1)                                       | 130(2)   | 130(2)   |
| radiation  | MoK $\alpha$                                   | MoK $\alpha$                                   | MoK $\alpha$                                   | MoK $\alpha$                                   | MoK $\alpha$                                   |
| wavelength (Å)   | 0.71073  | 0.71073  | 0.71073  | 0.71073  | 0.71073  |
| crystal system   | orthorhombic                                   | orthorhombic                                   | monoclinic                                     | orthorhombic                                   | monoclinic                                     |
| space group  | <i>Pnma</i>                                    | <i>Pbca</i>                                    | <i>P21/c</i>                                   | <i>Pnma</i>                                    | <i>P21/c</i>                                   |
| unit cell dimensions   |  |  |  |  |  |
| <i>a</i> (Å)   | 7.951(2)                                       | 7.812(1)                                       | 7.954(2)                                       | 8.229(1)                                       | 8.337(1)                                       |
| <i>b</i> (Å)   | 9.368(3)                                       | 18.612(2)                                      | 10.348(3)                                      | 9.537(1)                                       | 10.102(1)                                      |
| <i>c</i> (Å)   | 17.681(5)                                      | 19.912(2)                                      | 14.484(4)                                      | 17.916(2)                                      | 14.630(1)                                      |
| $\alpha$ (deg)   | 90   | 90   | 90   | 90   | 90   |
| $\beta$ (deg)  | 90   | 90   | 100.102(5)                                     | 90   | 106.140(1)                                     |
| $\gamma$ (deg)   | 90   | 90   | 90   | 90   | 90   |
| volume (Å <sup>3</sup> )                                     | 1317.0(6)                                      | 2895.1(5)                                      | 1173.8(5)                                      | 1406.2(3)                                      | 1183.6(2)                                      |
| <i>Z</i>   | 4  | 8  | 4  | 4  | 4  |
| <i>D<sub>c</sub></i> (Mg/m <sup>3</sup> )                    | 1.383  | 1.387  | 1.314  | 1.296  | 1.315  |
| $\mu$ (mm <sup>−1</sup> )                                    | 0.099  | 0.102  | 0.091  | 0.093  | 0.091  |
| <i>F</i> (000)   | 584  | 1280   | 496  | 584  | 504  |
| crystal size   | 0.40 × 0.40 × 0.50                             | 0.4 × 0.25 × 0.2                               | 0.40 × 0.30 × 0.15                             | 0.20 × 0.20 × 0.30                             | 0.20 × 0.20 × 0.30                             |
| $\theta$ range (deg)   | 2.30 to 25.00                                  | 2.05 to 25.00                                  | 2.00 to 25.00                                  | 2.27 to 25.00                                  | 2.52 to 24.99                                  |
| no. of refx collected  | 5956   | 12467  | 5875   | 5965   | 5783   |
| no. of independent refx                                      | 1203   | 2543   | 2077   | 1271   | 2073   |
| <i>R</i> (int)   | 0.0230   | 0.0711   | 0.0917   | 0.0539   | 0.0455   |
| obsd ( <i>I</i> > 2 $\sigma$ ( <i>I</i> ))                   | 1168   | 1874   | 713  | 1109   | 1796   |
| data/restraints/param  | 1203/0/100                                     | 2543/0/202                                     | 2077/0/158                                     | 1271/0/92                                      | 2073/0/158                                     |
| GOF on <i>F</i> <sup>2</sup>                                 | 1.245  | 1.002  | 0.732  | 1.031  | 1.060  |
| final <i>R</i> indices [ <i>I</i> > 2 $\sigma$ ( <i>I</i> )] | 0.0550   | 0.0479   | 0.0526   | 0.0359   | 0.0367   |
| <i>R</i> indices (all data)                                  | 0.0573   | 0.0699   | 0.1639   | 0.0404   | 0.0417   |
| weighting scheme <sup>a</sup>                                |  |  |  |  |  |
| <i>A</i>   | 0.042  | 0.063  | 0.03   | 0.063  | 0.045  |
| <i>B</i>   | 1.22   | 0  | 0  | 0.16   | 0.25   |
| largest diff peak and hole (eÅ <sup>−3</sup> )               | 0.222 and −0.368                               | 0.234 and −0.218                               | 0.207 and −0.131                               | 0.202 and −0.195                               | 0.217 and −0.175                               |

<sup>a</sup>  $w = 1/[\sigma^2(F_o^2) + (AP)^2 + BP]$ ; where  $P = (F_o^2 + 2F_c^2)/3$ .

TABLE 3. Selected Bond Lengths in 10–12, 14, and 16

| bond   | bond lengths (Å) |          |          |          |          |
|--------|------------------|----------|----------|----------|----------|
|        | 10               | 11       | 12       | 14       | 16       |
| C3–C9  | 1.518(4)         | 1.526(4) | 1.541(3) | 1.538(2) | 1.538(2) |
| C6–C10 | 1.518(4)         | 1.538(4) | 1.540(3) | 1.538(2) | 1.516(2) |
| C9–C10 | 1.438(4)         | 1.470(4) | 1.486(3) | 1.540(3) | 1.538(2) |
| C4–C5  | 1.400(4)         | 1.383(4) | 1.376(3) | 1.538(3) | 1.543(2) |
| C2–C7  | 1.379(4)         | 1.388(4) | 1.402(3) | 1.401(2) | 1.396(2) |
| C2–C3  | 1.489(3)         | 1.520(4) | 1.528(3) | 1.502(2) | 1.516(2) |
| C7–C6  | 1.489(3)         | 1.515(4) | 1.513(3) | 1.502(2) | 1.507(2) |
| C3–C4  | 1.511(4)         | 1.515(4) | 1.524(3) | 1.542(2) | 1.535(2) |
| C5–C6  | 1.511(4)         | 1.521(4) | 1.516(3) | 1.542(2) | 1.540(2) |

Crystal data and structure refinement details are summarized in Table 2 and selected bond distances are presented in Table 3. (Compounds **10** and **14** lie on a crystallographic plane of symmetry therefore a different atom labeling scheme is used. However, for comparison purposes the general numbering scheme in Table 3 is used.)

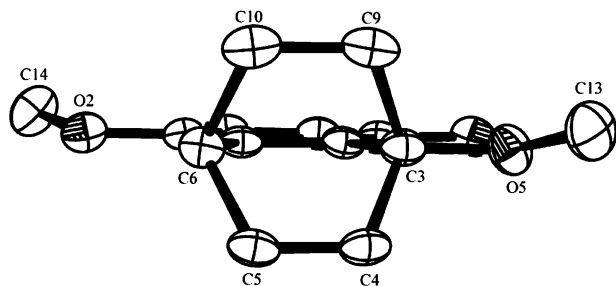
Inspection of the data for the bicyclo[2.2.2]octadiene derivatives **10–12** was confusing: the bonds from the bridgehead



FIGURE 1. The disordered orientation of the ethylene and ethyne bridges.

carbons to the ethylene fragment (bonds C<sub>3</sub>–C<sub>9</sub> and C<sub>6</sub>–C<sub>10</sub>) were not lengthened compared to those from the less reactive bicyclo[2.2.2]octene derivatives **14** and **16**. However, the C<sub>9</sub>–C<sub>10</sub> bond was significantly shorter than the corresponding CH<sub>2</sub>–CH<sub>2</sub> bond in **14** and **16**, while the C<sub>4</sub>–C<sub>5</sub> bond were significantly longer than a standard C=C double bond. The latter two effects are consistent with pronounced structural effects of the Alder–Rickert reaction, whereby C<sub>9</sub>–C<sub>10</sub> increases in bond order and C<sub>4</sub>–C<sub>5</sub> decreases in bond order. However, the absence of any significant lengthening of C<sub>3</sub>–C<sub>9</sub> and C<sub>6</sub>–C<sub>10</sub> bonds conflicts with this. The best explanation we can offer is that the structures are disordered over a pseudo-noncrystallographic mirror plane defined by the aromatic ring, and the bridgehead carbon with two orientations of the saturated and unsaturated 2-carbon bridges superimposed in the crystal lattice (Figure 1).

The appearance of this disorder suggests that the crystal-packing requirements of the two-carbon bridges CH<sub>2</sub>–CH<sub>2</sub> and CH=CH are similar, allowing for the two orientations to occur within the crystal. Evidence of this disorder can also be obtained by examining the thermal parameters for the carbons involved. In all three structures these carbons have larger thermal



**FIGURE 2.** The C<sub>9</sub> and C<sub>10</sub> ellipsoids extended along the C–C bond in **11**.

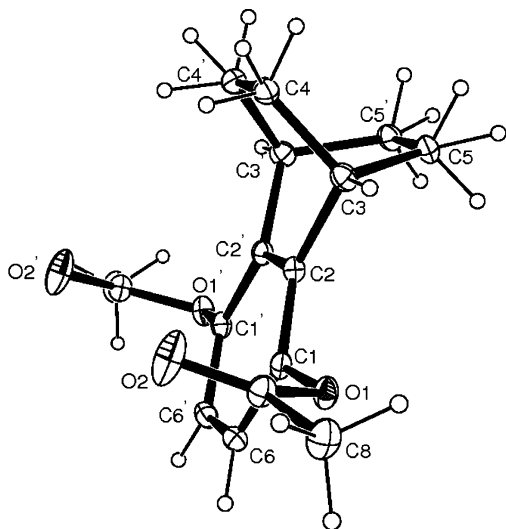


**FIGURE 3.** Thermal ellipsoid plot of **10** showing the disordered hydrogen atoms.

parameters than the remainder of the atoms in the molecule, and the ellipsoids are extended along the axis of the C–C bond consistent with overlap of two carbons with a C=C distance and two carbons with a C–C distance (Figure 2).

Difference electron densities were observed around the two bridges in all three compounds consistent with the presence of the disordered methylene and olefinic hydrogen atoms (Figure 3). These were included in the model with occupancies fixed at 50%.

This particular problem of disorder, which we propose arises due to the similar packing requirements of the CH<sub>2</sub>–CH<sub>2</sub> and CH=CH moieties, is removed in the partially reduced bicycloocta[2.2.2]octene derivatives **14** and **16**. It was interesting to observe that both **14** and **16** were isomorphous with **10** and **12** with slightly different unit cell dimensions reflecting the slightly different compositions. This provides further evidence for the similar crystal packing requirements of the CH<sub>2</sub>–CH<sub>2</sub> and CH=CH moieties. This disorder explains the lack of lengthening of C<sub>3</sub>–C<sub>9</sub> and C<sub>6</sub>–C<sub>10</sub> bonds, as these arise by superposition of these bonds with the C<sub>3</sub>–C<sub>4</sub> and C<sub>5</sub>–C<sub>6</sub> bonds, which being Csp<sup>2</sup>–Csp<sup>3</sup> bonds are naturally shorter. Unfortunately, this also means that the structural data provided by these structures are unreliable, and cannot be used in any further analysis. This result also calls into question the reliability of the parameters reported in the structures **6**–**8** which were extracted from the Cambridge Crystallographic database, for which this disorder is also likely to occur.

**TABLE 4.** Selected One-Bond <sup>13</sup>C–<sup>13</sup>C Coupling Constants for the Symmetrical Derivatives<sup>a</sup>

|                                   |             |             |             |
|-----------------------------------|-------------|-------------|-------------|
|                                   |             |             |             |
| (9)                               | (10)        | (19)        | (20)        |
|                                   |             |             |             |
| (13)                              | (14)        | (22)        | (23)        |
| <b>9</b>                          |             |             |             |
| <sup>1</sup> J <sub>CC</sub> (Hz) |             |             |             |
| a, b                              | 38.5        | 41.5        | 30.5 (–1.2) |
| c, d                              | 27.6 (–5.4) | 28.3 (–4.7) | 31.1 (–1.9) |
| <b>13</b>                         |             |             |             |
| <sup>1</sup> J <sub>CC</sub> (Hz) |             |             |             |
| a, b                              | 39.5        | 41.8        | 31.7        |
| c, d                              | 31.5 (–1.5) | 31.3 (–1.7) | 33.0        |

<sup>a</sup> Values in parentheses represent comparison with the model compound **22** and **23**.

<sup>a</sup> Values in parentheses represent comparison with the model compounds **22** and **23**.

**<sup>13</sup>C–<sup>13</sup>C One-Bond Coupling Constants.** While reliable structural information cannot be obtained for the bicyclo[2.2.2]octadiene derivatives in the solid state, information can be obtained in solution from measurement of <sup>13</sup>C–<sup>13</sup>C one-bond coupling constants. Unkefer stated that the one-bond <sup>13</sup>C–<sup>13</sup>C coupling constant is a useful basis for predicting bond lengths for those compounds where crystallographic data are unavailable, and demonstrated the existence of a linear but inverse relationship between bond length and coupling constant.<sup>15</sup> These are conveniently measured by using a 1D inadequate NMR experiment. This experiment suppresses the main uncoupled signal and yields only the satellites as antiphase multiplets whose difference in chemical shift provides the coupling constant <sup>1</sup>J<sub>CC</sub>.<sup>16,17</sup> By this method <sup>13</sup>C–<sup>13</sup>C coupling constants were determined for compounds **9**–**14**, and in addition **17**–**23**, which were required for comparison. Bicyclo[2.2.2]octene derivatives **17**–**20** were prepared by reaction between 1-methoxy-1,3-cyclohexadiene or 1,3-cyclohexadiene with maleic anhydride or *N*-methyl maleimide as dienophiles while bicyclo[2.2.2]octane derivatives **21**–**23** were obtained from catalytic hydrogenation of **18**–**20**.

Selected <sup>13</sup>C–<sup>13</sup>C coupling constants for **9**–**14** and **17**–**23** are presented in Tables 4 and 5. The <sup>13</sup>C–<sup>13</sup>C coupling constants for bonds labeled *c* and *d* in the model compounds **22** and **23** which cannot undergo the Alder–Rickert reaction are taken as “standard values” for comparison for the symmetrical derivatives **9**, **10**, **13**, **14**, **19**, and **20** while the model compound **21** provides standard <sup>13</sup>C–<sup>13</sup>C coupling constants for comparing bonds *c* and *d* in the unsymmetrical derivatives **11**, **12**, **17**, and **18**. The coupling constants for bonds *c* and *d* in the symmetrical model compounds **22** and **23** are similar and have an average value of 33 Hz, and the corresponding bonds for those symmetrical

(15) Unkefer, C. J.; London, R. E.; Whaley, T. W.; Daub, G. H. *J. Am. Chem. Soc.* **1983**, 105, 733–5.

(16) Jones, G. R.; Caldarelli, Vogel, P. *Helv. Chim. Acta* **1997**, 80, 59.

(17) Bax, A.; Freeman, R.; Kempell, S. P. *J. Magn. Reson.* **1980**, 41, 349.



**TABLE 5.** Selected One-Bond  $^{13}\text{C}$ – $^{13}\text{C}$  Coupling Constants for the Unsymmetrical Derivatives<sup>a</sup>

|                            | 11          | 12          | 17          | 18          | 21   |
|----------------------------|-------------|-------------|-------------|-------------|------|
| $^1J_{\text{CC}}$ (Hz)     |             |             |             |             |      |
| <i>a</i>                   | 43.8        | 43.5        | 34.1 (–2.2) | 34.6 (–1.7) | 36.3 |
| <i>b</i>                   | 40.0        | 40.1        | 30.7 (–2.3) | 32.1 (–0.9) | 33.0 |
| <i>c</i>                   | 32.7 (–4.1) | 33.0 (–3.8) | 35.2 (–1.6) | 35.2 (–1.6) | 36.8 |
| <i>d</i>                   | 27.9 (–5.2) | 27.3 (–5.8) | 30.5 (–2.6) | 31.3 (–1.8) | 33.1 |
| $\text{CH}_2\text{--CH}_2$ | 38.5 (+3.5) | 40.4 (+6.4) | 36.0 (+2.0) | 35.8 (+1.8) | ~34  |

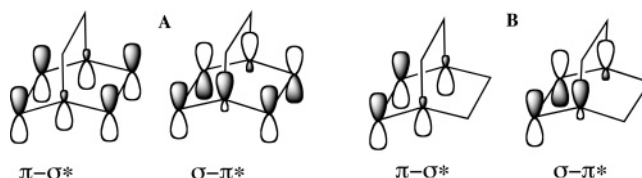
<sup>a</sup> Values in parentheses represent comparison with the model compound **21**. (The value for  $\text{CH}_2\text{--CH}_2$  in **21** is approximate due to partial overlap.)

derivatives **9**, **10**, **13**, **14**, **19**, and **20** which can potentially undergo the Alder–Rickert reaction have coupling constants which are significantly decreased, consistent with bond weakening in the ground state.

In the reactive symmetrical bicyclooctadienes **9** and **10** (for which extrusion of ethylene results in the formation of an aromatic ring), the coupling constants for bonds *c* and *d* are decreased by 5.4 and 4.7 Hz, respectively, compared with the model compound. The slightly larger effect observed for **9** is consistent with the greater reactivity of this system. The effects on the corresponding coupling constants in the less reactive bicyclooctenes **13**, **14**, **19**, and **20**, which are decreased by 1.5, 1.7, 1.9, and 1.9 Hz, respectively, relative to **22** and **23**, are significantly less. Thus a relationship between relative bond distance (as implied by the  $^{13}\text{C}$ – $^{13}\text{C}$  coupling constant) and reactivity is established. Cycloadducts **19** and **20** can undergo an alternative retro-Diels–Alder reaction with the breaking of bonds *a* and *b* resulting in fragmentation to cyclohexadiene and maleic anhydride or *N*-methyl maleimide, and the  $^{13}\text{C}$ – $^{13}\text{C}$  coupling constants for these bonds are decreased by 1.2 and 1.3 Hz compared to **22** and **23**, respectively, consistent with manifestation of this alternative pathway in the ground state.<sup>5</sup>

The  $^{13}\text{C}$ – $^{13}\text{C}$  coupling constants for bonds *a* and *c* in the unsymmetrical derivatives **11**, **12**, **17**, **18**, and **21** are 3–4 Hz larger than those similar bonds in the symmetrical derivatives, which is consistent with the expected effects of the electronegative methoxy substituent.<sup>18</sup> In the reactive unsymmetrical bicyclooctadienes **11** and **12** the  $^{13}\text{C}$ – $^{13}\text{C}$  coupling constants for bond *c* are decreased by 4.1 and 3.8 Hz, respectively, compared with the model **21**, while bond *d* has decreased by 5.2 and 5.8 Hz, respectively. In the less reactive unsymmetrical bicyclooctenes **17** and **18**, the  $^{13}\text{C}$ – $^{13}\text{C}$  coupling constants are decreased by 1.6 Hz for bond *c* and 2.6 and 1.8 Hz, respectively, for bond *d*. Again a relationship between the relative bond length (as implied by the relative  $^{13}\text{C}$ – $^{13}\text{C}$  coupling constants) and the reactivity is demonstrated. The  $^{13}\text{C}$ – $^{13}\text{C}$  coupling constants for the ethylene bridge in **11**, **12**, **17**, and **18** also show systematic trends; compared to the model system **21**, these are significantly greater in the reactive derivatives **11** and **12** (4.5 and 6.4 Hz, respectively) suggesting the development of some double-bond character; a smaller increase is seen for the less reactive derivatives **17** and **18** (2.0 and 1.8 Hz, respectively).

(18) Marshall, J. L. In *Carbon–Carbon and Carbon–Proton NMR Couplings*; Marchand, A. P., Ed.; Verlag Chemie International: Deerfield Beach, FL, 1983; pp 65–218.

**FIGURE 4.** Hyperconjugative orbital interactions in the bicyclooctadiene (A) and bicyclooctene (B) frameworks.

For cycloadducts **17** and **18** which can also undergo the alternative retro-Diels–Alder reaction with breaking of bonds *a* and *b*, these bonds have  $^{13}\text{C}$ – $^{13}\text{C}$  coupling constants which are 2.2 and 1.7 Hz smaller, respectively, than those for the model system **21** for bond *a* and 2.3 and 0.9 Hz smaller, respectively, for bond *b*, again demonstrating the manifestation of this alternative reaction pathway in the ground state.

## Conclusion

These results clearly demonstrate that the Alder–Rickert ethylene extrusion reaction manifests in the ground state structures of molecules containing the bicyclo[2.2.2]octadiene and bicyclo[2.2.2]octene moieties. A significant decrease of the  $^{13}\text{C}$ – $^{13}\text{C}$  one-bond coupling constants for the C–C bonds, which break in this fragmentation reaction, suggests lengthening, and hence weakening of these bonds. In the unsymmetrical systems these effects are also shown to be associated with strengthening of the  $\text{CH}_2\text{--CH}_2$  bond, which is ultimately lost from the molecule as ethylene. The magnitude of these effects is also clearly dependent on the reactivity of the molecule toward this reaction, with larger effects observed for **9**, **10** and **11** and **12**, which give rise to an aromatic product upon loss of ethylene.

The origins of the structural effects implied in the bicyclooctadiene and bicyclooctene derivatives have their genesis in the orbital interactions in Figure 4. It is these same interactions which facilitate the Alder–Rickert reaction: these are examples of normal ( $\sigma\text{--}\pi^*$ ) and negative hyperconjugation ( $\pi\text{--}\sigma^*$ ). The extra structural effects observed for the bicyclooctadiene derivatives are readily understood by reference to Figure 4.

## Experimental Section

**1. X-ray Crystallography.** Intensity data were collected with a Bruker SMART Apex CCD detector, using Mo K $\alpha$  radiation (graphite crystal monochromator  $\lambda = 0.71073$ ). Data were reduced by using the program SAINT. The temperature during data collection was maintained at 130.0(1) °C with an Oxford Cryostream cooling device. The structures were solved by direct methods and difference Fourier synthesis. Thermal ellipsoid plots were generated with the program ORTEP-3<sup>19</sup> integrated within the WINGX<sup>20</sup> suite of programs.

**2. Synthesis.** 1,3-Cyclohexadiene, 1,4-benzoquinone, 1-methoxycyclohexa-1,3-diene, maleic anhydride, and *N*-methylmaleimide were purchased reagent grade from commercial sources. All reactions were carried out in oven-dried glassware under nitrogen atmosphere. Solvents were redistilled prior to use in moisture-sensitive reactions according to literature procedures.<sup>21</sup> Melting points were determined on a capillary melting point apparatus and are uncorrected.  $^1\text{H}$  and  $^{13}\text{C}$  NMR spectra were recorded as solutions in deuterated chloroform on 300, 400, and 500 MHz spectrometers.

(19) Farrugia, L. J. *J. Appl. Crystallogr.* **1997**, *30*, 565.

(20) Farrugia, L. J. *J. Appl. Crystallogr.* **1999**, *32*, 837.

(21) Perrin, D. D.; Armarego, W. L. F. *Purification of Laboratory Chemicals*, 3rd ed.; Pergamon Press: New York, 1988.

$^1\text{H}$  spectra were referenced to residual chloroform at  $\delta$  7.26 ppm and the signals are reported as chemical shift (ppm) followed by (in brackets) integration, multiplicity, coupling constant, and peak assignment.  $^{13}\text{C}$  spectra were referenced to residual chloroform at  $\delta$  77.0 ppm and the signals are reported as chemical shift (ppm) followed by (in brackets) the peak assignment. Cyclooctyne was prepared according to Meier et al.<sup>12</sup> and compounds **19**, **20**, **22**, and **23** were previously reported.<sup>5</sup>

**Tricyclo[8.2.2.0<sup>2,9</sup>]tetradec-2,11-diene (9).** 1,3-Cyclohexadiene (0.5 mL, 0.421 g, 5.25 mmol) was added to cyclooctyne (1.143 g, 10.6 mmol) and the mixture was stirred under mild reflux (60–70 °C) for 24 h. The mixture was washed with chloroform (ca. 5 mL), concentrated under reduced pressure, and purified via short path distillation (0.1–0.3 mbar, 60–70 °C) to yield **9** as a yellow oil (0.228 g, 1.21 mmol, 23%).  $^1\text{H}$  NMR ( $\text{CDCl}_3$ )  $\delta$  6.14 (2H, t,  $J$  = 3.7 Hz,  $\text{CH}=\text{CH}$ ), 3.26 (2H, br s,  $\text{CH}-\text{CH}_2$ ), 2.26 (4H, m,  $\text{CH}_2$ ), 1.61 (4H, m,  $\text{CH}_2$ ), 1.20–1.56 (8H, m,  $\text{CH}_2$ );  $^{13}\text{C}$  NMR ( $\text{CDCl}_3$ )  $\delta$  137.9 ( $\text{CH}-\text{C}=\text{C}$ ), 134.3 ( $\text{HC}=\text{CH}$ ), 43.1 ( $\text{CH}-\text{CH}_2$ ), 30.1 ( $\text{CH}_2$ ), 28.8 ( $\text{CH}_2$ ), 26.1 ( $\text{CH}_2$ ), 25.2 ( $\text{CH}-\text{CH}_2$ ).

**Tricyclo[8.2.2.0<sup>2,9</sup>]tetradec-2-ene (13).** **9** (0.228 g, 1.21 mmol) was dissolved in methanol (10 mL) and the solution was stirred over palladium/charcoal (5%) in a hydrogen environment for 24 h. The solid was filtered and the filtrate was concentrated under reduced pressure to afford **13** as a pale yellow oil (0.218 g, 1.15 mmol, 95%).  $^1\text{H}$  NMR ( $\text{CDCl}_3$ )  $\delta$  2.30 (2H, t,  $J$  = 5.0 Hz,  $\text{C}-\text{CH}-\text{CH}_2$ ), 1.53–1.25 (12H, s,  $\text{CH}_2$ ), 1.67 (8H, d,  $J$  = 5.6 Hz,  $\text{CH}_2$ );  $^{13}\text{C}$  NMR ( $\text{CDCl}_3$ )  $\delta$  136.9 ( $\text{HC}=\text{CH}$ ), 36.2 ( $\text{CH}-\text{CH}_2$ ), 30.7 ( $\text{CH}_2$ ), 29.5 ( $\text{CH}_2$ ), 26.6 ( $\text{CH}-\text{CH}_2$ ), 26.5 ( $\text{CH}_2$ ).

**5,8-Diacetoxy-1,4-dihydro-1, 4-ethanonaphthalene (10).** 1,3-Cyclohexadiene (2.4 mL, 2.02 g, 25.4 mmol) was added to 1,4-benzoquinone (1.212 g, 11.3 mmol) dissolved in dichloromethane (10 mL) and the solution was allowed to stir for 48 h in a nitrogen environment. The solvent was removed under reduced pressure and the yellow powder was dissolved in dry acetone (5 mL) and potassium carbonate (0.5 g) was added. The mixture was stirred under reflux in a nitrogen environment for 2 h. The mixture was cooled, filtered, and concentrated under reduced pressure. Acetic anhydride (0.69 mL, 7.32 mmol) and pyridine (6.37 mL, 4.91 mmol) were added and the solution was refluxed for 3 h in a nitrogen atmosphere. The solution was cooled and poured into excess water and the red precipitate was dissolved and extracted into diethyl ether (20 mL). The solution was filtered through a pack of silica (3 cm) and the column was rinsed by diethyl ether (100 mL). The filtrate was concentrated under reduced pressure and recrystallized from chloroform/petroleum spirit (1:1) to yield **10** as colorless crystals (0.226 g, 0.829 mmol, 62%). Mp 141–143 °C (lit.<sup>13</sup> mp 180 °C);  $^1\text{H}$  NMR ( $\text{CDCl}_3$ )  $\delta$  6.77 (2H, s), 6.44 (2H, dd,  $J$  = 4.49, 3.12 Hz), 3.99 (2H, br s), 2.35 (6H, s), 1.49 (4H, s);  $^{13}\text{C}$  NMR ( $\text{CDCl}_3$ )  $\delta$  169.2, 142.0, 137.5, 134.5, 118.6, 34.3, 24.3, 20.6.

**5,8-Diacetoxy-1,4-ethano-1,2,3,4-tetrahydronaphthalene (14).** **10** (0.201 g, 0.739 mmol) was dissolved in methanol (10 mL) and the solution was stirred over palladium/charcoal (5%) in a hydrogen environment for 24 h. The solid was filtered and the filtrate was concentrated under reduced pressure. The residue was recrystallized from chloroform to afford **14** as colorless crystals (0.186 g, 0.679 mmol, 92%). Mp 116–119 °C;  $^1\text{H}$  NMR ( $\text{CDCl}_3$ )  $\delta$  6.83 (2H, s), 2.99 (2H, s), 2.27 (6H, s), 1.67 (4H, d,  $J$  = 7.42 Hz), 1.35 (4H, d,  $J$  = 7.42 Hz);  $^{13}\text{C}$  NMR ( $\text{CDCl}_3$ )  $\delta$  169.0, 142.7, 137.0, 118.9, 27.8, 24.8, 20.6.

**5,8-Diacetoxy-1,4-ethano-1,4-dihydro-1-methoxynaphthalene (11).** A solution of 1-methoxycyclohexa-1,3-diene (7.692 g, 0.045 mol) and 1,4-benzoquinone (4.421 g, 0.040 mol) in dry benzene (50 mL) was refluxed under a nitrogen atmosphere for 4 h. The solvent was evaporated to give an oily residue to which was added dry acetone (100 mL) and potassium carbonate (12 g). The mixture was stirred vigorously under reflux in a nitrogen atmosphere for 2 h, cooled, filtered, and concentrated under reduced pressure. Acetic anhydride (18.007 g, 0.176 mmol) and pyridine (13.997 g, 0.177 mmol) were added and the solution was refluxed

for 3 h in a nitrogen atmosphere. The mixture was then poured into water, and solid was collected from filtration and purified with column chromatography, using ethyl acetate/petroleum spirit (3:7) as eluent, to afford **11** as colorless blocks (8.5 g, 28.1 mmol, 70%). Mp 144–145 °C (lit.<sup>13</sup> mp 147–148 °C);  $^1\text{H}$  NMR ( $\text{CDCl}_3$ )  $\delta$  6.85 (1H, d,  $J$  = 8 Hz), 6.65 (1H, d,  $J$  = 8.0 Hz), 6.55–6.25 (2H, m), 3.95–3.75 (1H, m), 3.55 (3H, s), 2.24 (3H, s), 2.33 (3H, s), 1.8–1.4 (4H, m);  $^{13}\text{C}$  NMR ( $\text{CDCl}_3$ )  $\delta$  169.8, 169.1, 141.9, 136.4, 136.0, 134.8, 132.6, 120.4, 119.5, 83.5, 53.5, 33.6, 28.5, 25.1, 20.6, 20.6.

**1,4-Ethano-1,4-dihydro-8-hydroxy-1,5-dimethoxynaphthalene (12).** A solution of 1-methoxy-1,3-cyclohexadiene (1.421 g, 13.0 mmol) and 1,4-benzoquinone (0.982 g, 9.0 mmol) in dry benzene (20 mL) was heated under reflux in a nitrogen atmosphere until no trace of 1,4-benzoquinone was observed by thin layer chromatography (2.5 h) and solvent was evaporated under reduced pressure. Dry acetone (20 mL), potassium carbonate (10.0 g) and iodomethane (2.84 g, 0.020 mol) were added to the residue and the mixture was stirred vigorously under reflux in a nitrogen atmosphere for 20 h, cooled, and filtered. The residue obtained by evaporation of the solvent was purified by column chromatography with ethyl acetate/petroleum spirit (1:9) as eluent to afford **12**, which was recrystallized from dichloromethane/petroleum spirit to give block crystals (1.44 g, 6.2 mmol, 68%). Mp 87–88 °C (lit.<sup>14</sup> mp 90–91 °C).  $^1\text{H}$  NMR ( $\text{CDCl}_3$ )  $\delta$  8.7 (1H, s), 6.66 (1H, d,  $J$  = 8.2 Hz), 6.59 (2H, m), 6.49 (1H, dd,  $J$  = 8.8, 5.3 Hz), 4.35 (1H, d,  $J$  = 5.6 Hz), 3.8 (3H, s), 3.7 (3H, s), 1.4–1.9 (4H, m);  $^{13}\text{C}$  NMR ( $\text{CDCl}_3$ )  $\delta$  146.2, 134.2, 134.0, 130.9, 127.3, 112.9, 109.9, 85.7, 55.9, 51.5, 32.0, 27.8, 25.2.

**5,8-Diacetoxy-1,4-ethano-1,2,3,4-tetrahydro-1-methoxynaphthalene (15).** **11** (0.230 g, 0.761 mmol) was dissolved in methanol (10 mL) and the solution was stirred over palladium/charcoal (5%) in a hydrogen environment for 24 h. The solid was filtered and the filtrate was concentrated under reduced pressure. The residue was recrystallized from chloroform to afford **15** as colorless crystals (0.206 g, 0.685 mmol, 90%). Mp 119–121 °C;  $^1\text{H}$  NMR ( $\text{CDCl}_3$ )  $\delta$  6.92 (1H, d,  $J$  = 8.8 Hz), 6.82 (1H, d,  $J$  = 8.5 Hz), 3.4 (3H, s), 2.96 (1H, br s), 2.32 (3H, s), 2.27 (3H, s), 1.89–1.79 (4H, m), 1.66 (2H, t,  $J$  = 10.1 Hz), 1.53 (2H, t,  $J$  = 10.5 Hz);  $^{13}\text{C}$  NMR ( $\text{CDCl}_3$ )  $\delta$  170.1, 169.5, 142.6, 142.5, 136.4, 135.6, 121.1, 120.0, 78.2, 51.6, 28.6, 27.6, 25.3, 20.8, 20.7.

**1,4-Ethano-1,2,3,4-tetrahydro-8-hydroxy-1,5-dimethoxynaphthalene (16).** **12** (0.205 g, 0.883 mmol) was dissolved in methanol (10 mL) and the solution was stirred over palladium/charcoal (5%) in a hydrogen environment for 24 h. The solid was filtered and the filtrate was concentrated under reduced pressure. The residue was recrystallized from chloroform to afford **16** as colorless crystals (0.184 g, 0.785 mmol, 89%). Mp 117–119 °C;  $^1\text{H}$  NMR ( $\text{CDCl}_3$ )  $\delta$  6.70 (1H, d,  $J$  = 9.0 Hz), 6.40 (1H, d,  $J$  = 8.8 Hz), 3.75 (3H, s), 3.48 (3H, s), 3.40 (1H, s), 2.18 (2H, t,  $J$  = 9.7 Hz), 1.84 (2H, t,  $J$  = 11.9 Hz), 1.55–1.45 (4H, m);  $^{13}\text{C}$  NMR ( $\text{CDCl}_3$ )  $\delta$  147.0, 146.5, 131.1, 126.3, 113.2, 110.7, 81.6, 56.3, 49.2, 49.1, 27.7, 25.8, 25.4.

**1-Methoxycyclohexa-1,3-diene Maleic Anhydride Cycloadduct (17).** Maleic anhydride (0.29 g, 2.96 mmol) and 1-methoxy-1,3-cyclohexadiene (0.44 g, 4.01 mmol) in diethyl ether (100 mL) were reacted at room temperature for 3 days. The crude product was recrystallized from diethyl ether to give **17** as colorless crystals (0.49 g, 2.35 mmol, 79%). Mp 86–88 °C (lit.<sup>22</sup> mp 87–89 °C);  $^1\text{H}$  NMR ( $\text{CDCl}_3$ )  $\delta$  6.31 (2H, m), 3.48 (3H, s), 3.33–3.09 (3H, m), 1.64 (4H, m);  $^{13}\text{C}$  NMR ( $\text{CDCl}_3$ )  $\delta$  172.2, 169.1, 135.2, 131.1, 77.8, 51.0, 46.0, 45.9, 31.4, 26.3, 24.1.

**1-Methoxycyclohexa-1,3-diene N-Methylmaleimide Cycloadduct (18).** N-Methylmaleimide (0.371 g, 3.33 mmol) and 1-methoxy-1,3-cyclohexadiene (0.560 g, 5.09 mmol) were dissolved in toluene (10 mL) and heated at 70 °C for 5 h. Evaporation of the solvent under reduced pressure, followed by column chromatog-

(22) Brown, R. S.; Marcinko, R. W. *J. Am. Chem. Soc.* **1978**, *100*, 5721–7.

raphy of the residue on silica with hexane/chloroform (2:1) as eluent, gave **18** as brown waxy solid (0.589 g, 2.67 mmol, 80%). Mp 87–89 °C (lit.<sup>23</sup> mp 87–88 °C); <sup>1</sup>H NMR (CDCl<sub>3</sub>) δ 5.99–5.89 (2H, m), 3.41 (3H, s), 3.11 (1H, m), 3.09 (1H, d, *J* = 8.19 Hz), 2.96 (1H, dd, *J* = 2.96, 8.19 Hz), 2.80 (3H, s), 1.85–1.66 (2H, m), 1.59–1.45 (2H, m); <sup>13</sup>C NMR (CDCl<sub>3</sub>) δ 177.6, 175.3, 133.9, 129.8, 77.8, 50.3, 44.9, 44.5, 26.5, 23.9, 23.8.

**Reduced 1-Methoxycyclohexa-1,3-diene *N*-Methylmaleimide Cycloadduct (21).** A mixture of cycloadduct **18** (0.500 g, 2.26 mmol) and 5% palladium on carbon (120 mg) in methanol (25 mL) was stirred under hydrogen at room temperature and atmospheric pressure. After consumption of 1 molar equiv of hydrogen (60 mL), the reaction mixture was filter through celite and solvent was removed under reduced pressure. The crude product was dissolved in chloroform and filter through a silica plug to give **21** as pale yellow needles. Mp 98–99 °C (0.42 g, 1.90 mmol, 84%); <sup>1</sup>H NMR-

(CDCl<sub>3</sub>) δ 3.20 (3H, s), 3.08 (1H, m), 3.01 (1H, m), 2.89 (3H, m), 2.18 (1H, m), 1.90–1.76 (3H, m), 1.69–1.60 (3H, m), 1.50–1.56 (1H, m), 1.43–1.39 (1H, m); <sup>13</sup>C NMR (CDCl<sub>3</sub>) δ 179.1, 176.7, 74.1, 49.4, 45.7, 44.2, 27.7, 26.9, 26.0, 25.8, 24.5, 22.4.

**Acknowledgment.** Our gratitude goes to the University of Melbourne for MIRS and MIFRS scholarships, and the Albert Shimmins Fund award to Goh Yit Wooi.

**Supporting Information Available:** CIF files for **9–11** and copies of NMR spectra. This material is available free of charge via the Internet at <http://pubs.acs.org>. CCDC 640219–640223 contain the supplementary crystallographic data for this paper. These data can be obtained free of charge via [www.ccdc.cam.ac.uk/data\\_request/cif](http://www.ccdc.cam.ac.uk/data_request/cif), by e-mailing [data\\_request@ccdc.cam.ac.uk](mailto:data_request@ccdc.cam.ac.uk), or by contacting The Cambridge Crystallographic Data Centre, 12, Union Road, Cambridge CB2 1EK; fax +44 1233 336033.

JO0625610

(23) Hu, Z.; Lakshmikantham, M. V.; Cava, M. P.; Becher, J.; Hansen, T.; Jorgensen, T. *J. Org. Chem.* **1992**, *57*, 3988–90.